International Journal of Modern Physics E
Vol. 23, No. 12 (2014) 1450084 (22 pages)

DOI: 10.1142/S0218301314500840

On transverse momentum spectra of negative pions in ^{12}C+^{181}Ta collisions at 4.2A GeV/c

Khusniddin K. Olimov

Department of Physics,
COMSATS Institute of Information Technology,
45550, Park Road, Islamabad, Pakistan

Physical-Technical Institute of
Uzbek Academy of Sciences,
100084, Tashkent, Uzbekistan
olimov@comsats.edu.pk

Akhtar Iqbal

Department of Physics,
COMSATS Institute of Information Technology,
45550, Park Road, Islamabad, Pakistan

S. L. Lutpullaev

Physical-Technical Institute of Uzbek Academy of Sciences,
100084, Tashkent, Uzbekistan
lutp@uzsci.net

Imran Khan

Department of Physics, Gomal University,
Dera Ismail Khan, Pakistan

Viktor V. Glagolev

Laboratory of High Energies,
Joint Institute for Nuclear Research, 141980, Dubna, Russia

Mahnaz Q. Haseeb

Department of Physics,
COMSATS Institute of Information Technology,
45550, Park Road, Islamabad, Pakistan
mahnazhaseeb@comsats.edu.pk

Received 5 July 2014
Revised 17 November 2014
Accepted 18 November 2014
Published 17 December 2014

We studied the dependences of the experimental transverse momentum spectra of the negative pions, produced in minimum bias ^{12}C+^{181}Ta collisions at a momentum of 4.2 GeV/c per nucleon, on the collision centrality and the pion rapidity range. To examine quantitatively, the change in the shape of the p_t spectra of π^-mesons with the change of collision centrality and the pion rapidity range, all the extracted p_t spectra were fitted by the four different functions commonly used for describing the hadron spectra. The extracted values of the spectral temperatures T_1 and T_2 were consistently larger for the p_t spectra of π^- mesons coming from midrapidity range as compared to those of the negative pions generated in the target and projectile fragmentation regions. The spectral temperatures of the negative pions coming from projectile fragmentation region proved to be larger than the respective temperatures of the negative pions coming from target fragmentation region. The extracted spectral temperatures T_1 and T_2 of the p_t spectra of π^- mesons were compatible within the uncertainties for the peripheral, semicentral and central ^{12}C+^{181}Ta collision events, selected using the number of participant protons. It was observed that Hagedorn and Boltzmann functions are more appropriate for describing the transverse momentum spectra of the negative pions as contrasted to Simple Exponential and Gaussian functions.

Keywords: Relativistic nucleus–nucleus collisions; pions; spectral temperatures of hadrons; transverse momentum distribution of hadrons; Hagedorn thermodynamic model; Boltzmann function.

PACS Number(s): 14.40.Be, 25.75.Dw

1. Introduction

In relativistic nucleus–nucleus collisions, the temperature and density of nuclear matter are amongst the main parameters of the nuclear equation of the state (EOS). To estimate the spectral temperatures of the secondary hadrons, the slopes of the energy or transverse momentum spectra of these hadrons are usually analyzed. Most of the energy spent on particle production during relativistic nuclear collision is used for pion production. Therefore, the investigation of the properties of pions, produced most abundantly in relativistic nuclear collisions, is necessary to understand the dynamics of the nuclear collisions. The negatively-charged pions are produced predominantly at the energies of the Dubna synchrophasotron and can be unambiguously separated from the other particles formed in nuclear collisions. The excitation and decay of baryon resonances are believed to be the main processes responsible for pion production in relativistic nuclear collisions. It was shown in Refs. 1–9 that significant fraction of pions produced in experiments on 2 m propane and 1 m hydrogen bubble chambers of Joint Institute for Nuclear Research (JINR, Dubna, Russia) originated from decay of Δ resonances. The decay kinematics of Δ resonances was shown to be responsible for low transverse momentum enhancement of pion spectra in hadron–nucleus and nucleus–nucleus collisions at incident beam energies from 1 GeV to 15 GeV per nucleon.[9–11] It was found that pions coming from Δ decay populated mainly the low transverse momentum part of the p_t spectra of pions.[9–11]

In Ref. 12, the spectral temperatures of π^-mesons produced in d+^{12}C, ^{4}He+^{12}C and ^{12}C+^{12}C collisions at 4.2 A GeV/c were obtained by fitting the noninvariant

center-of-mass (cms) energy spectra of π^-mesons with Maxwell–Boltzmann distribution function. Analysis of rapidity and angular dependences of the spectral temperatures of the negative pions produced in ^{12}C+^{12}C collisions at $4.2A\,\mathrm{GeV}/c$ was done in Ref. 13. The temperatures of the negative pions have been extracted and analyzed for collisions of different sets of nuclei at various energies in the past.[12,14–18] Analysis of transverse momentum as well as transverse mass distributions is preferred for estimating the hadron temperatures, due to their Lorentz invariance with respect to longitudinal boosts.[14,17,19,20] Hence, transverse momentum distributions have much lesser likelihood of getting affected by the longitudinal collective motion as contrasted to the energy spectra of hadrons.

The present work continues the analyses of our recent papers[13,20–22] devoted to investigation of various characteristics of π^-mesons produced in nucleus–nucleus collisions at $4.2\,\mathrm{GeV}/c$ per nucleon. The main aim of the present paper is to study the dependences of the experimental transverse momentum spectra of the negative pions, produced in ^{12}C+^{181}Ta collisions at a momentum of $4.2\,\mathrm{GeV}/c$ per nucleon, on the collision centrality as well as on the pion rapidity range. To examine quantitatively, the change in the shape of the p_t spectra of π^-mesons in ^{12}C+^{181}Ta collisions with the change of the collision centrality and pion rapidity range, all the extracted p_t spectra were fitted by four different functions commonly used for describing the hadron spectra. It is also of interest to check which of these commonly used functions would be more appropriate for fitting the transverse momentum spectra of the negative pions. It is necessary to mention that the similar analysis of the transverse momentum spectra of the negative pions produced in symmetric ^{12}C+^{12}C collisions at $4.2A\,\mathrm{GeV}/c$ for different collision centralities and various pion rapidity ranges was also done in our recent paper.[22]

2. Experimental Procedures and Analysis

The data analyzed in the present work were obtained using 2 m propane (C_3H_8) bubble chamber of the Laboratory of High Energies of JINR (Dubna, Russia). The 2 m propane bubble chamber was in a magnetic field of strength 1.5 T[23–30] and three tantalum (^{181}Ta) foils were placed in the experimental setup of the chamber. Thickness of each foil was 1 mm and the separation distance between the foils was 93 mm. The bubble chamber was then irradiated with beams of ^{12}C nuclei accelerated to a momentum of $4.2\,\mathrm{GeV}/c$ per nucleon at Dubna synchrophasotron. Methods of selection of inelastic ^{12}C+^{181}Ta collision events in this experiment were given in detail in Refs. 23–30. Threshold for detection of π^-mesons produced in ^{12}C+^{181}Ta collisions was about $80\,\mathrm{MeV}/c$. In some momentum and angular intervals, the particles could not be detected with 100% efficiency. To account for small losses of particles emitted under large angles to object plane of the camera and due to tantalum foils, the relevant corrections were introduced as discussed in Refs. 23–30. The average uncertainty in measurement of emission angle of the negative pions was 0.8°. The mean relative uncertainty of momentum measurement of

π^-mesons from the curvature of their tracks in propane bubble chamber was 6%. All the negative particles, except those identified as electrons, were considered to be π^-mesons. Admixtures of unidentified electrons and negative strange particles among them were less than 5%. In our experiment, the spectator protons are protons with momenta $p > 3\,\mathrm{GeV}/c$ and emission angle $\theta < 4^\circ$ (projectile spectators), and protons with momenta $p > 0.3\,\mathrm{GeV}/c$ (target spectators) in the laboratory frame.[23–30] These criteria are based on the fact that, having spin-1/2, nucleons in nuclei posses Fermi momentum. Thus, practically all the spectator nucleons have momenta $p_n < p^F_{\max}$, where $p^F_{\max}$ is the maximum Fermi momentum in the nucleus rest frame, which is around 0.2–0.3 GeV/c for carbon and tantalum nuclei, taking into account the mean relative uncertainty of momentum measurement of protons $\langle\frac{\Delta p}{p}\rangle \approx 11\%$ in the present experiment. Hence, the participant protons are the protons which remain after elimination of the spectator protons. Statistics of the experimental data analyzed in the present work consist of 2420 ^{12}C+^{181}Ta minimum bias inelastic collision events with almost all the secondary-charged particles detected and measured with 4π acceptance.

Comparison of the mean multiplicities per event of the negative pions and participant protons and the average values of rapidity and transverse momentum of π^- mesons in ^{12}C+^{181}Ta collisions at 4.2 GeV/c per nucleon, both in the experiment and Quark–Gluon-String-Model (QGSM)[31–34] is presented in Table 1. QGSM was developed to describe hadron–nucleus and nucleus–nucleus collisions at high energies. In the QGSM, hadron production occurs via formation and decay of quark–gluon strings. This model is used as a basic process for generation of hadron–hadron collisions. In the present work, the version of QGSM[32] adapted to the range of intermediate energies ($\sqrt{s_{nn}} \leq 4\,\mathrm{GeV}$) was used. The incident momentum of 4.2 GeV/c per nucleon for the collisions analyzed in the present work corresponds to incident kinetic energy 3.37 GeV per nucleon and nucleon–nucleon cms energy $\sqrt{s_{nn}} = 3.14\,\mathrm{GeV}$.

The QGSM is based on Regge and string phenomenology of particle production in inelastic binary hadron collisions. To describe the evolution of the hadron and quark–gluon phases, a coupled system of Boltzmann-like kinetic equations was used in the model. The nuclear collisions were treated as a superposition of independent interactions of the projectile and target nucleons, stable hadrons and short lived resonances. Resonant reactions like $\pi + N \to \Delta$, pion absorption by NN quasi-deuteron

Table 1. Mean multiplicities per event of the negative pions and participant protons and the average values of rapidity and transverse momentum of π^- mesons in ^{12}C+^{181}Ta collisions at 4.2 GeV/c per nucleon. The mean rapidities are calculated in cms of nucleon–nucleon collisions at 4.2 GeV/c. Only statistical errors are given here and at tables that follow.

Type	$\langle n(\pi^-)\rangle$	$\langle n_{\mathrm{part.prot.}}\rangle$	$\langle y_{\mathrm{c.m.}}(\pi^-)\rangle$	$\langle p_t(\pi^-)\rangle$, GeV/$c$
Exper	3.50 ± 0.10	13.3 ± 0.2	-0.34 ± 0.01	0.217 ± 0.002
QGSM	5.16 ± 0.09	14.4 ± 0.2	-0.38 ± 0.01	0.191 ± 0.001

pairs and also $\pi + \pi \rightarrow \rho$ were taken into account in this model. The time of formation of hadrons were also included in QGSM. The masses of strings at intermediate energies are very small. At cms energy $\sqrt{s_{nn}} = 3.14\,\text{GeV}$ the masses of strings are smaller than 2 GeV, and these strings fragment predominantly (∼90%) through two-particle decay channel.

The nucleon coordinates in the colliding nuclei were generated, according to the realistic nuclear matter density. The sphere of the nucleus was filled with the nucleons subject to the condition that the distance between nucleons was greater than 0.8 fm. The Fermi motion of the nucleons inside the nucleus was taken into account in the model. The nucleon momenta p_N were distributed in the range $0 \leq p_N \leq p_F$, where p_F is the maximum Fermi momentum of a nucleon for a given nucleus, determined by its nuclear density. The procedure of generation of a collision event in QGSM consisted of three steps: (i) defining the configurations of the colliding nucleons; (ii) production of quark–gluon strings; (iii) the breakup (fragmentation) of strings into observed hadrons. For simulating the nucleon–nucleon and pion–nucleon interactions in QGSM, the binary, "undeveloped" cylindrical, diffractive, cylindrical and planar topological quark diagrams were used.[23–26] The binary processes give the main contribution to QGSM and correspond to a quark rearrangement (in interacting pair of nucleons) without direct particle emission in the string decay. This process mainly results in resonance production (for example, in reactions $p + n \rightarrow p + \Delta^0, p + p \rightarrow n + \Delta^{++}, n + n \rightarrow p + \Delta^-, n + n \rightarrow n + \Delta^0$, etc), and the resonances are the main source of pion production in QGSM.

The transverse momenta of pions produced in quark–gluon string fragmentation processes are the product of two factors: (i) string motion on the whole as a result of transverse motion of constituent quarks and (ii) $q\bar{q}$-pair production from breakup of the string. Transverse motion of quarks inside hadrons was described by the Gaussian distribution with variance $\sigma^2 \approx 0.3\ (\text{GeV}/c)^2$. The transverse momentum k_T of produced $q\bar{q}$ quark pairs in the cms of the string was defined according to a distribution $W(k_T) = \frac{3b}{\pi(1+bk_T^2)^4}$, where $b = 0.34\,(\text{GeV}/c)^{-2}$. For hadron interactions, the cross-sections were taken from the experimental data. Isotopic invariance and predictions of the additive quark model (for meson–meson cross-sections, etc.) were used to avoid data deficiency. The resonance interaction cross-sections were taken to be equal to the interaction cross-sections of stable particles with the same quark content. The decay of excited recoil nuclear fragments and coupling of nucleons inside the nucleus were not taken into account in QGSM.

The total transverse momentum and rapidity distributions of the negative pions in minimum bias $^{12}\text{C}+^{181}\text{Ta}$ collisions at a momentum of 4.2 GeV/c per nucleon are shown in Fig. 1. As seen from Fig. 1(a), the experimental transverse momentum spectrum of π^- mesons is described satisfactorily by the QGSM calculations. The rapidity spectrum in Fig. 1(b) is plotted in cms of nucleon–nucleon collisions at 4.2 GeV/c (the rapidity of the cms of nucleon–nucleon collision is $y_{\text{cms}} \approx 1.1$ at this incident momentum). Figure 1(a) also shows that the QGSM slightly underestimates the experimental p_t spectrum of π^- mesons in region $p_t > 0.8\,\text{GeV}/c$.

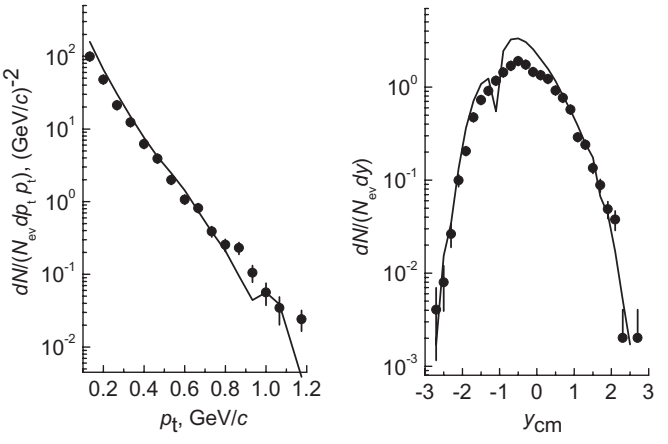

(a) (b)

Fig. 1. The experimental transverse momentum (a) and rapidity (b) spectra of negative pions produced in minimum bias ^{12}C+^{181}Ta (•) collisions at 4.2 GeV/c per nucleon. The corresponding calculated QGSM spectra are given by the solid lines. All the spectra are normalized per one inelastic collision event.

It is worth mentioning that another model — Modified FRITIOF model,[24,35–37] specifically designed for describing the nucleus–nucleus collisions at incident energies of the order of a few GeV per nucleon, also underestimates this high p_t part of the pion spectra.[20,38] It was observed earlier[20] that the fitting of the p_t spectrum of π^- in d+^{12}C, ^{4}He+^{12}C and ^{12}C+^{12}C collisions at 4.2A GeV/c with the two-temperature Hagedorn function resulted in the lower spectral temperatures T_1 and T_2 for both QGSM and Modified FRITIOF model spectra as compared to the experimental ones. As seen from Fig. 1(b), QGSM describes satisfactorily the experimental rapidity spectrum of π^- mesons in ^{12}C+^{181}Ta collisions.

However, as can be seen from Fig. 1(b), the double peak structure is observed in QGSM rapidity spectrum of the negative pions in ^{12}C+^{181}Ta collisions. The appearance of this structure in the model is likely due to separation of heavy target fragmentation region from the central rapidity region in ^{12}C+^{181}Ta collisions, whereas the central rapidity and projectile fragmentation regions overlap with each other due to their relative closeness in the rapidity space. The absence of such a structure in the experimental rapidity distribution is obviously due to the experimental broadening caused by the experimental resolution of the rapidity spectrum. Therefore, the target fragmentation and central rapidity regions overlap in the experimental rapidity distribution of the negative pions. As seen from Fig. 1(a), the kink structure is observed in the region $p_t \approx 0.9$–1.0 GeV/c of the QGSM transverse momentum spectrum of the negative pions. The appearance of this structure is most probably due to the statistical fluctuations caused by the fact that, in the model only very few pions are produced in the region $p_t > 0.9$–1.0 GeV/c and

the QGSM spectrum ends at the lower p_t values compared to the experimental transverse momentum spectrum of the negative pions.

In the present analysis, we fitted the transverse momentum spectra of π^-mesons produced in ^{12}C+^{181}Ta collisions at a momentum of 4.2 GeV/c per nucleon by four different functions commonly used for describing the p_t spectra of hadrons. The Hagedorn Thermodynamic Model[19,39] allows for a set of fireballs displaced from each other in rapidity. In this model, particles with different momenta freeze out within a volume that is of universal magnitude when assessed in the rest frame for any given momentum, being the distribution in transverse momentum of the shape $dN/dp_t = \text{const.}\cdot p_t \cdot m_t \cdot K_1(m_t/T) \approx \text{const.}\cdot p_t \cdot (m_t \cdot T)^{1/2} \cdot \exp(-m_t/T)$, where K_1 is the MacDonald function, $m_t = \sqrt{m^2 + p_t^2}$ is the transverse mass, T is the spectral temperature. The above approximation is valid for $m_t \gg T$. Thus, Hagedorn Thermodynamic Model[19,39] predicts that the normalized transverse momentum (p_t) distribution of hadrons can be described using the expression (assuming $m_t \gg T$)

$$\frac{dN}{Np_t dp_t} = A \cdot (m_t T)^{1/2} \exp\Big(-\frac{m_t}{T}\Big), \tag{1}$$

where N (depending on the choice of normalization) is either the total number of inelastic events or the total number of the respective hadrons and A is the fitting constant. This relation (1) will be referred to as the one-temperature Hagedorn function throughout the present paper. Correspondingly, in case of two temperatures, T_1 and T_2, the above formula is modified as

$$\frac{dN}{Np_t dp_t} = A_1 \cdot (m_t T_1)^{1/2} \exp\left(-\frac{m_t}{T_1}\right) + A_2 \cdot (m_t T_2)^{1/2} \exp\left(-\frac{m_t}{T_2}\right), \tag{2}$$

referred to as the two-temperature Hagedorn function in this work.

The Boltzmann Model assumes that the transverse momentum spectra of hadrons can be fitted using m_t Boltzmann distribution function given by

$$\frac{dN}{Np_t dp_t} = A m_t \exp\Big(-\frac{m_t}{T}\Big), \tag{3}$$

referred as the one-temperature Boltzmann function in the present paper. In case of two temperatures, T_1 and T_2, the above formula is modified as

$$\frac{dN}{Np_t dp_t} = A_1 \cdot m_t \exp\left(-\frac{m_t}{T_1}\right) + A_2 \cdot m_t \exp\left(-\frac{m_t}{T_2}\right). \tag{4}$$

The spectra of pions can also be described using the Simple Exponential function as follows for the one-temperature and two-temperature scenarios, respectively:

$$\frac{dN}{Np_t dp_t} = A \exp\Big(-\frac{p_t}{T}\Big) \tag{5}$$

and

$$\frac{dN}{Np_t dp_t} = A_1 \cdot \exp\left(-\frac{p_t}{T_1}\right) + A_2 \cdot \exp\left(-\frac{p_t}{T_2}\right). \tag{6}$$

Another possibility for describing the transverse momentum spectra of hadrons could be the Gaussian function given below for the one-temperature and the two-temperature cases as

$$\frac{dN}{Np_t dp_t} = A \exp\left(-\frac{p_t^2}{T^2}\right) \tag{7}$$

and

$$\frac{dN}{Np_t dp_t} = A_1 \cdot \exp\left(-\frac{p_t^2}{T_1^2}\right) + A_2 \cdot \exp\left(-\frac{p_t^2}{T_2^2}\right), \tag{8}$$

respectively.

We fitted the total transverse momentum spectra of the negative pions in the whole range of p_t in ^{12}C+^{181}Ta collisions at $4.2A\,\mathrm{GeV}/c$ by the two-temperature and the one-temperature Hagedorn and Boltzmann functions. The experimental transverse momentum spectra of the negative pions produced in minimum bias ^{12}C+^{181}Ta collisions at $4.2A\,\mathrm{GeV}/c$ per nucleon and the corresponding fits in the whole p_t range by the one-temperature and the two-temperature Hagedorn functions are given in Fig. 2. As can be seen from Fig. 2, the two-temperature Hagedorn function fits the total p_t spectra of the negative pions very well as compared to the one-temperature fit. Parameters extracted from fitting the total transverse momentum spectra of the negative pions in the whole range of p_t in ^{12}C+^{181}Ta collisions at $4.2A\,\mathrm{GeV}/c$ by the two-temperature and the one-temperature Hagedorn and Boltzmann functions are given in Table 2. It is necessary to mention that R^2 factor in Table 2 is defined as $R^2 = 1 - \frac{SS_E}{SS_T}$, where $SS_E = \sum_{i=1}^{n}(y_i^{\mathrm{exp}} - y_i^{\mathrm{fit}})^2$ is the sum of squared errors, $SS_T = \sum_{i=1}^{n}(y_i^{\mathrm{exp}} - \bar{y})^2$ is the total sum of squares, y_i^{exp} and y_i^{fit} are

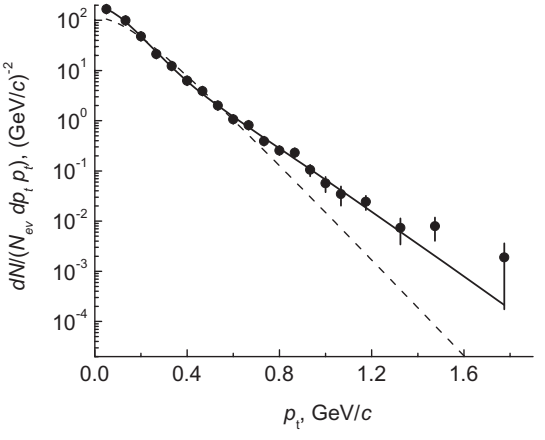

Fig. 2. The experimental transverse momentum spectra (•) of the negative pions produced in minimum bias ^{12}C+^{181}Ta collisions at $4.2\,\mathrm{GeV}/c$ per nucleon and the corresponding fits in the whole p_t range by the one-temperature (dashed line) and the two-temperature (solid line) Hagedorn functions. All the spectra are normalized per one inelastic collision event.

Table 2. The parameters extracted from fitting the total transverse momentum spectra of negative pions in the whole range of p_t in $^{12}C+^{181}Ta$ collisions at $4.2A\,GeV/c$ by the two-temperature and the one-temperature Hagedorn and Boltzmann functions.

Fitting function	A_1 $(GeV)^{-1}$	T_1 (MeV)	A_2 $(GeV)^{-1}$	T_2 (MeV)	$\chi 2$/n.d.f.	R^2 factor
Two temperature Hagedorn	$21{,}715 \pm 4335$	57 ± 3	494 ± 149	128 ± 6	0.93	0.99
One temperature Hagedorn	5040 ± 391	88 ± 1	—	—	7.79	0.92
Two temperature Boltzmann	$19{,}069 \pm 3229$	50 ± 2	385 ± 98	116 ± 5	1.02	0.99
One temperature Boltzmann	4296 ± 322	78 ± 1	—	—	10.03	0.89

the original (experimental) and fit (model) data, respectively, and $\bar{y} = \frac{1}{n}\sum_{i=1}^{n} y_i^{\exp}$ is the mean value of the experimental data. As the deviation between the experimental and fit data gets smaller, R^2 factor approaches to 1. Thus, the closer R^2 factor value to 1, the better is the fit quality. As can be seen from comparison of χ^2/n.d.f. and R^2 factor values in Table 2, the two-temperature Hagedorn and the two-temperature Boltzmann function fits describe the experimental spectra much better as compared to the one-temperature fits. This is in agreement with our recent papers[13,20] and earlier works,[12,14,16,17] where the transverse momentum as well as energy spectra of pions, produced in relativistic nuclear collisions, were characterized by the two-temperature shapes. In early work,[14] the two-temperature shape of cm kinetic energy spectra of the negative pions in Ar+KCl collisions at 1.8 GeV/nucleon was obtained. In this work the occurrence of two temperatures, T_1 and T_2, was interpreted as due to two channels of pion production: pions coming from Δ resonance decay (T_1) and directly produced pions (T_2). In Ref. 16, the two-temperature shape of kinetic energy spectrum of pions emitted at 90° in cms of central La+La collisions at 1.35 GeV/nucleon was interpreted as due to different contributions of deltas originated from the early and later stages of heavy-ion reactions. The two-temperature behavior was also observed for cm energy as well as p_t spectra of π^-mesons produced in Mg+Mg collisions[17] at incident momentum of 4.2–4.3$A\,GeV/c$.

It would be oversimplified to believe that the origin of pions in a minimum bias sample of $^{12}C+^{181}Ta$ collisions could be described by two thermal sources. The phenomenon of collective flow has become the well-established and an important feature of relativistic heavy-ion collisions. Inverse slope parameter, T, or an apparent temperature of the emitting source, of transverse mass spectra of hadrons was shown to consist of two components: a thermal part, $T_{\rm thermal}$ and a second part resembling the collective expansion with an average transverse velocity $\langle\beta_t\rangle$.[40] It is necessary to mention that the collective flow of protons and negative pions was also observed experimentally in He+C, C+C, C+Ne, C+Cu and C+Ta collisions within the momentum range of 4.2–4.5$A\,GeV/c$.[27,41,42] Hence, the observed two-temperature shape of the transverse momentum spectrum of the negative pions produced in $^{12}C+^{181}Ta$ collisions at $4.2A\,GeV/c$ could also be interpreted by the collective flow effects.

Table 3. The spectral temperatures (T) of the negative pions in ^{12}C+^{181}Ta collisions at $4.2A$ GeV/c and their relative contributions (R) extracted in the present work from fitting their total transverse momentum spectra in the whole range of p_t by the two-temperature Hagedorn and Boltzmann functions compared to the corresponding values obtained in Ref. 12 from fitting the noninvariant cm energy spectra of the negative pions by Maxwell–Boltzmann distribution function for ^{12}C+^{181}Ta collisions at $4.2A$ GeV/c.

Fitting function	T_1 (MeV)	R_1%	T_2 (MeV)	R_2%	$\chi 2$/n.d.f.	R^2 factor
Hagedorn	57 ± 3	80 ± 22	128 ± 6	20 ± 7	0.92	0.99
Boltzmann	50 ± 2	83 ± 20	116 ± 5	17 ± 5	1.02	0.99
Maxwell–Boltzmann	66 ± 2	88 ± 3	159 ± 6	12 ± 3	0.58	—

The spectral temperatures (T_1, T_2) of π^- mesons in ^{12}C+^{181}Ta collisions at $4.2A$ GeV/c and their relative contributions (R_1, R_2) extracted in the present work from fitting the p_t spectra by the two-temperature Hagedorn and the two-temperature Boltzmann functions are presented in Table 3. The corresponding results obtained in Ref. 12 from fitting the noninvariant cm energy spectra of the negative pions in ^{12}C+^{181}Ta collisions at the same initial momentum using two-temperature Maxwell–Boltzmann distribution function are also shown for a comparison in this table. The relative contributions, R, of the different temperatures to the total negative pion multiplicity were calculated over the total transverse momentum interval ($R_i = c_i/(c_1 + c_2)$, where $c_i = A_i \cdot \int (m_t T_i)^{1/2} \exp(-\frac{m_t}{T_i}) dp_t$ and $c_i = A_i \cdot \int m_t \exp(-\frac{m_t}{T_i}) dp_t$ $(i = 1, 2)$ are for the case of Hagedorn and Boltzmann function fits, respectively). It should be mentioned that the statistics of ^{12}C+^{181}Ta collisions used in Ref. 12 was 1989 inelastic collisions, which is about 20% lesser compared to the statistics used in the present analysis. As seen from Table 3, the values of the spectral temperatures (T_1, T_2) extracted in the present work from fitting the p_t spectra by the two-temperature Hagedorn and the two-temperature Boltzmann functions proved to be noticeably lower compared to the corresponding values obtained in Ref. 12 from fitting the noninvariant cm energy spectra of negative pions by Maxwell–Boltzmann distribution for ^{12}C+^{181}Ta collisions at $4.2A$ GeV/c. Especially, the value of T_2 obtained in Ref. 12 seems to be quite high for such relatively small collision energy. This is likely due to the influence of longitudinal motion on the energy spectra of π^- mesons, whereas p_t spectra are Lorentz invariant with respect to longitudinal boosts. As seen from Table 3, the dominant contribution ($R_1 \sim$ 80–83%) to the total π^- multiplicity in ^{12}C+^{181}Ta collisions is given by $T_1 \sim (50\text{–}57) \pm 3$ MeV, which is compatible within the uncertainties with the results of the Ref. 12. It is worth mentioning that the fits by Boltzmann function give slightly lower values of the spectral temperatures compared to those by Hagedorn function.

It is evident from Fig. 2 that the p_t spectrum of the negative pions with $p_t \leq 1.2$ GeV/c is characterized by a good enough statistics of π^- and therefore by sufficiently low statistical errors. Due to the lower momentum threshold of detection of pions $p_{\text{thresh}} \approx 80$ MeV/c, it is natural to fit the transverse momentum spectra of

the pions in the range $p_t = 0.1$–$1.2\,\mathrm{GeV}/c$, where pions are detected and measured with almost 100% efficiency. We fitted the transverse momentum spectra of π^- in this p_t range in minimum bias $^{12}\mathrm{C}+^{181}\mathrm{Ta}$ collisions at $4.2A\,\mathrm{GeV}/c$ by different two-temperature functions given in expressions (2), (4), (6) and (8). Parameters extracted from fitting the total transverse momentum spectra of the negative pions in the range $p_t = 0.1$–$1.2\,\mathrm{GeV}/c$ in $^{12}\mathrm{C}+^{181}\mathrm{Ta}$ collisions at $4.2A\,\mathrm{GeV}/c$ by different two-temperature functions are presented in Table 4. As seen from Tables 2 and 4, the values of T_1 and T_2 obtained from fitting the p_t spectra of the negative pions in the range $p_t = 0.1$–$1.2\,\mathrm{GeV}/c$ by the two-temperature Hagedorn and Boltzmann functions are compatible within the uncertainties with the corresponding temperature values extracted from fitting in the whole p_t range. It is observed from Table 4 that the fits by Hagedorn and Boltzmann functions give reasonably acceptable values for T_1 and T_2 with quite small values of χ^2/n.d.f. The fitting with Simple Exponential function leads to significantly higher values of T_1 and T_2 compared to the fits with Hagedorn and Boltzmann functions. Moreover, the fitting with Gaussian function results in too large and unphysical values of T_1 and T_2 with quite high value of χ^2/n.d.f.

The experimental transverse momentum spectrum of the negative pions produced in minimum bias $^{12}\mathrm{C}+^{181}\mathrm{Ta}$ collisions at $4.2\,\mathrm{GeV}/c$ per nucleon and the corresponding fits in the range $p_t = 0.1$–$1.2\,\mathrm{GeV}/c$ by the two-temperature Hagedorn and the two-temperature Boltzmann functions are presented in Fig. 3. As seen from Fig. 3, the two-temperature Hagedorn and the two-temperature Boltzmann functions fit very well the p_t spectrum of the negative pions in $^{12}\mathrm{C}+^{181}\mathrm{Ta}$ collisions.

It is of interest to analyze quantitatively the change in the shape of transverse momentum spectra of the pions with increase in the collision centrality, which corresponds to decrease of the impact parameter of collision. Since impact parameter is not directly measurable, we use the number of participant protons to characterize the collision centrality. We follow Refs. 20, 23, 43 and 44 to define the peripheral collision events to be those in which $N_p \leq \langle n_{\mathrm{part.prot}} \rangle$, and the central collisions as the collision events with $N_p \geq 2\langle n_{\mathrm{part.prot}} \rangle$, where $\langle n_{\mathrm{part.prot}} \rangle$ is the mean multiplicity per event of participant protons and the semicentral collisions come in between

Table 4. The parameters extracted from fitting the total transverse momentum spectra of the negative pions in the range $p_t = 0.1$–$1.2\,\mathrm{GeV}/c$ in $^{12}\mathrm{C}+^{181}\mathrm{Ta}$ collisions at $4.2A\,\mathrm{GeV}/c$ by various two-temperature functions. (The units of A_1 and A_2 are $(\mathrm{GeV})^{-1}$ in case of Hagedorn and Boltzmann function fits and dimensionless in case of Simple exponential and Gaussian function fits wherever appropriate in the tables that follow.)

Fitting function	A_1	T_1 (MeV)	A_2	T_2 (MeV)	$\chi 2$/n.d.f.	R^2 factor
Hagedorn	$28{,}312 \pm 10{,}614$	53 ± 5	641 ± 204	123 ± 6	0.91	0.99
Boltzmann	$21{,}121 \pm 6359$	49 ± 3	449 ± 127	113 ± 5	1.02	0.99
Simple exponential	417 ± 72	76 ± 10	67 ± 35	144 ± 12	0.73	0.99
Gaussian	8 ± 1	436 ± 11	121 ± 10	196 ± 6	3.03	0.97

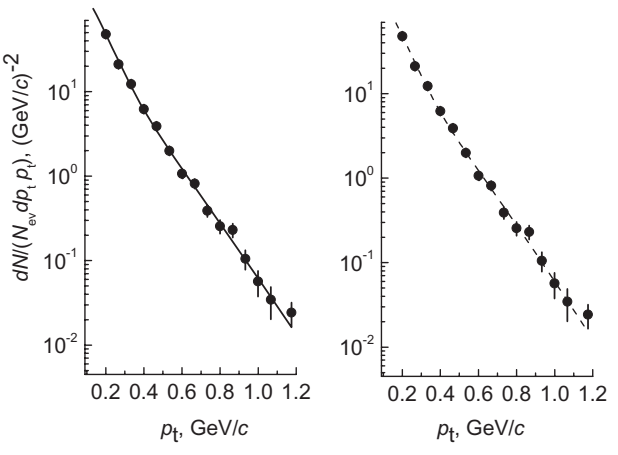

Fig. 3. The experimental transverse momentum spectrum of the negative pions produced in minimum bias ^{12}C+^{181}Ta (•) collisions at 4.2 GeV/c per nucleon and the corresponding fits in the range p_t = 0.1–1.2 GeV/c by the two-temperature Hagedorn (solid line) and the two-temperature Boltzmann (dashed line) functions. All the spectra are normalized per one inelastic collision event.

these two multiplicity regions. It was shown in Ref. 43 that the central ^{12}C+^{181}Ta collisions at 4.2A GeV/c selected using the above criterion were characterized by complete projectile stopping, because in these collisions the average number of interacting projectile nucleons (the average number of participant nucleons from projectile nucleus) was very close to the total number of nucleons in projectile carbon. Fractions of central, semicentral and peripheral ^{12}C+^{181}Ta collision events, relative to the total inelastic cross-section, obtained for both experimental and QGSM data are presented in Table 5. As seen from Table 5, the experimental and corresponding model fractions of peripheral and central ^{12}C+^{181}Ta collision events coincide with each other within the two standard errors. However, the fraction of semicentral ^{12}C+^{181}Ta collisions is slightly overestimated by QGSM.

We fitted the p_t spectra of the negative pions in peripheral, semicentral and central ^{12}C+^{181}Ta collision events in the range p_t = 0.1–1.2 GeV/c by the above two-temperature functions given in expressions (2), (4), (6) and (8). The parameters extracted from fitting the transverse momentum spectra of the negative pions in the range p_t = 0.1–1.2 GeV/c in peripheral, semicentral and central ^{12}C+^{181}Ta

Table 5. Fractions of central, semicentral and peripheral ^{12}C+^{181}Ta collisions at 4.2 GeV/c per nucleon relative to the total inelastic cross-section.

	Peripheral collisions (%)		Semicentral collisions (%)		Central collisions (%)	
Type	Experiment	QGSM	Experiment	QGSM	Experiment	QGSM
^{12}C+^{181}Ta	60 ± 2	56 ± 1	24 ± 1	29 ± 1	16 ± 1	15 ± 1

Table 6. The parameters extracted from fitting the transverse momentum spectra of the negative pions in the range $p_t = 0.1$–$1.2\,\mathrm{GeV}/c$ in peripheral, semicentral and central $^{12}\mathrm{C}+^{181}\mathrm{Ta}$ collisions at $4.2A\,\mathrm{GeV}/c$ by various two-temperature functions.

Fitting function	Collision centrality	A_1	T_1 (MeV)	A_2	T_2 (MeV)	$\chi 2$/n.d.f.	R^2 factor
Hagedorn	Peripheral	6214 ± 2326	63 ± 7	138 ± 101	139 ± 16	0.85	0.99
	Semicentral	$74{,}329 \pm 53{,}202$	46 ± 7	1766 ± 629	112 ± 6	0.50	0.99
	Central	$93{,}566 \pm 49{,}847$	49 ± 6	1624 ± 740	119 ± 8	1.11	0.98
Boltzmann	Peripheral	5465 ± 1785	56 ± 5	120 ± 71	123 ± 12	0.93	0.98
	Semicentral	$50{,}087 \pm 27{,}017$	44 ± 5	1196 ± 398	104 ± 5	0.49	0.99
	Central	$67{,}136 \pm 28{,}885$	46 ± 4	1138 ± 468	109 ± 7	1.17	0.98
Simple exponential	Peripheral	146 ± 19	95 ± 10	6 ± 10	193 ± 58	0.65	0.99
	Semicentral	714 ± 364	60 ± 18	220 ± 90	126 ± 9	0.55	0.99
	Central	1146 ± 285	71 ± 12	159 ± 108	140 ± 16	1.01	0.98
Gaussian	Peripheral	4 ± 1	441 ± 22	48 ± 5	202 ± 9	2.04	0.97
	Semicentral	20 ± 3	404 ± 13	213 ± 25	180 ± 8	0.86	0.99
	Central	22 ± 4	414 ± 17	326 ± 38	182 ± 8	2.27	0.96

collisions at $4.2A\,\mathrm{GeV}/c$ by various two-temperature functions are given in Table 6. As seen from Table 6, the fits of the p_t spectra by the two-temperature Hagedorn and the two-temperature Boltzmann functions are compatible with each other within the errors for peripheral, semicentral and central $^{12}\mathrm{C}+^{181}\mathrm{Ta}$ collisions. However the values of T_1 and T_2 extracted from fitting by Simple Exponential and Gaussian functions are significantly larger as compared to those obtained from fitting by the two-temperature Hagedorn and the two-temperature Boltzmann functions. As observed from Table 6, the absolute values of T_1 and T_2 extracted for peripheral collisions proved to be noticeably higher compared to those for semicentral and central collisions, though these temperatures are compatible within two standard errors for peripheral, semicentral and central collisions. This result could be understood if we recall that the temperature is the measure of the mean kinetic energy of particles and that we have highly asymmetric collision system with the target tantalum nuclei much heavier than light projectile carbon nuclei ($A_{\mathrm{proj}} \ll A_{\mathrm{target}}$). In case of central $^{12}\mathrm{C}+^{181}\mathrm{Ta}$ collisions, each of incoming projectile nucleons invokes at least several nucleon–nucleon collisions (interactions) with heavy target nucleons, which results in significantly higher multiplicity of pions produced on tantalum nuclei in central $^{12}\mathrm{C}+^{181}\mathrm{Ta}$ collisions as compared to peripheral $^{12}\mathrm{C}+^{181}\mathrm{Ta}$ collisions, where significantly lesser pions are produced, mostly in the first single collisions (interactions) of projectile nucleons with target nucleons. Indeed, as was shown in Fig. 1(b), the significantly larger number of pions is produced in heavy target fragmentation region as compared to light projectile fragmentation region. Thus, in case of central $^{12}\mathrm{C}+^{181}\mathrm{Ta}$ collisions, the collision energy is distributed among significantly larger number of pions compared to peripheral $^{12}\mathrm{C}+^{181}\mathrm{Ta}$ collisions, which results in lower mean kinetic energies of the negative pions in central $^{12}\mathrm{C}+^{181}\mathrm{Ta}$ collisions as compared to the peripheral ones.

The experimental transverse momentum spectra of the negative pions produced in peripheral, semicentral and central ^{12}C+^{181}Ta collisions at 4.2 GeV/c per nucleon and the corresponding fits in the range $p_t = 0.1$–1.2 GeV/c by the two-temperature Boltzmann function are given in Fig. 4.

As observed from Fig. 4(a), the p_t spectra of the negative pions for the central and semicentral ^{12}C+^{181}Ta collisions are located considerably above the corresponding spectrum for the peripheral ^{12}C+^{181}Ta collisions. This is obviously due to the known fact that, with an increase in the collision centrality, the number of nucleon–nucleon collisions and, hence, the number of the participant nucleons and produced pions increase. As can be seen from Fig. 4, the two-temperature Boltzmann function again fits very well the p_t spectra of the negative pions in peripheral, semicentral and central ^{12}C+^{181}Ta collisions.

It seems interesting also to analyze quantitatively the change in the shape of transverse momentum spectra of the negative pions with the change in the pion rapidity range. Therefore, we extracted and fitted, using the above two-temperature functions, the transverse momentum spectra of the negative pions for three different rapidity intervals in the nucleon–nucleon cms at 4.2 GeV/c: $y_{\rm cm} \leq -0.3$, $|y_{\rm cm.}| \leq 0.3$ and $y_{\rm cm.} \geq 0.3$, which can roughly be classified as target fragmentation, midrapidity and projectile fragmentation regions, respectively. The parameters extracted from fitting the transverse momentum spectra of the negative pions in the range p_t = 0.1–1.2 GeV/c in ^{12}C+^{181}Ta collisions at 4.2A GeV/c by various two-temperature

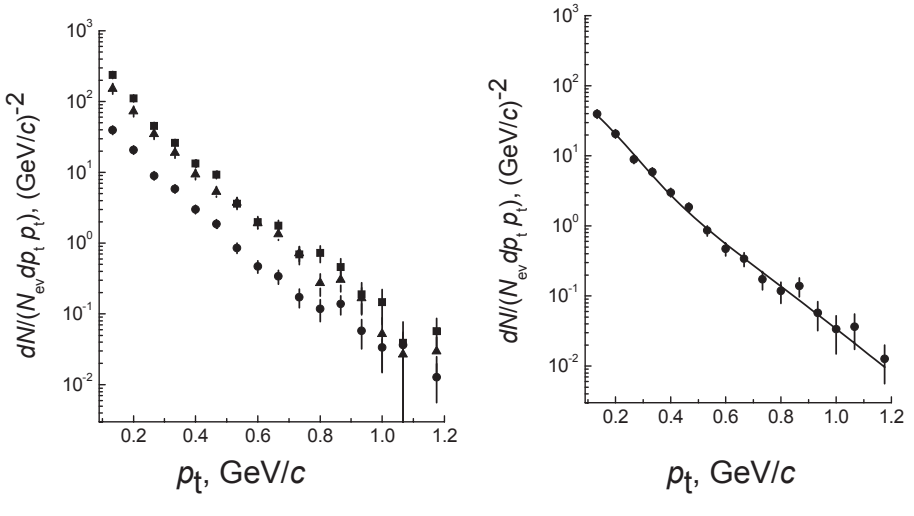

(a) (b)

Fig. 4. The experimental transverse momentum spectra of the negative pions produced in peripheral (•) ((a) and (b)), semicentral (▲) ((a) and (c)) and central (■) ((a) and (d)) ^{12}C+^{181}Ta collisions at 4.2 GeV/c per nucleon and the corresponding fits in the range p_t = 0.1–1.2 GeV/c by the two-temperature Boltzmann function (solid lines). All the spectra are normalized per one inelastic collision event.

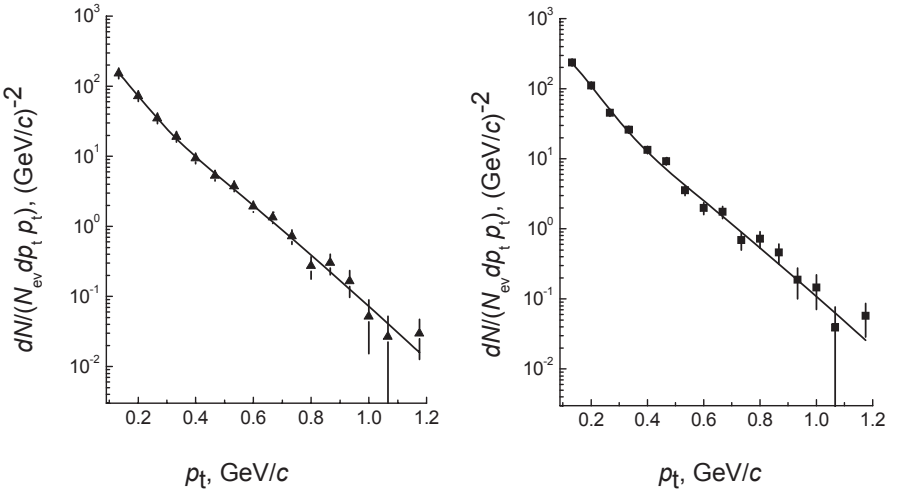

Fig. 4. (*Continued*)

Table 7. Parameters extracted from fitting the transverse momentum spectra of the negative pions in the range $p_t = 0.1$–$1.2\,\mathrm{GeV}/c$ in $^{12}\mathrm{C}+^{181}\mathrm{Ta}$ collisions at $4.2A\,\mathrm{GeV}/c$ by various two-temperature functions for different pion rapidity intervals.

Fitting function	Rapidity range	A_1	T_1 (MeV)	A_2	T_2 (MeV)	$\chi 2$/n.d.f.	R^2 factor
Hagedorn	$y_{\mathrm{cm.}} \leq -0.3$	$18{,}533 \pm 7825$	48 ± 4	247 ± 96	119 ± 7	1.46	0.98
	$\lvert y_{\mathrm{cm.}} \rvert \leq 0.3$	5556 ± 3859	56 ± 11	337 ± 162	122 ± 9	0.62	0.99
	$y_{\mathrm{cm.}} \geq 0.3$	9183 ± 6549	53 ± 11	415 ± 303	111 ± 12	0.76	0.99
Boltzmann	$y_{\mathrm{cm.}} \leq -0.3$	$13{,}521 \pm 4778$	44 ± 3	183 ± 64	108 ± 6	1.58	0.98
	$\lvert y_{\mathrm{cm.}} \rvert \leq 0.3$	4478 ± 2210	52 ± 7	229 ± 98	113 ± 7	0.61	0.99
	$y_{\mathrm{cm.}} \geq 0.3$	7475 ± 4182	48 ± 7	296 ± 185	102 ± 10	0.77	0.99
Simple exponential	$y_{\mathrm{cm.}} \leq -0.3$	211 ± 36	73 ± 8	17 ± 11	150 ± 17	1.16	0.99
	$\lvert y_{\mathrm{cm.}} \rvert \leq 0.3$	65 ± 27	80 ± 43	46 ± 40	137 ± 18	0.68	0.99
	$y_{\mathrm{cm.}} \geq 0.3$	121 ± 37	85 ± 26	27 ± 56	136 ± 40	0.76	0.99
Gaussian	$y_{\mathrm{cm.}} \leq -0.3$	4 ± 1	391 ± 13	62 ± 6	171 ± 6	3.31	0.96
	$\lvert y_{\mathrm{cm.}} \rvert \leq 0.3$	4 ± 1	442 ± 17	36 ± 4	204 ± 10	0.90	0.99
	$y_{\mathrm{cm.}} \geq 0.3$	6 ± 1	373 ± 18	49 ± 6	178 ± 11	1.16	0.98

functions for different pion rapidity intervals are displayed in Table 7. As can be seen from Table 7, the absolute values of T_1 and T_2 proved to be consistently larger for the midrapidity region compared to the target and projectile fragmentation regions in case of all the fitting functions used here, except for the Simple Exponential function. However, as observed from Table 7, the extracted values of T_1 and T_2 are compatible with each other within the errors for the analyzed three rapidity regions of the negative pion spectra. It can be noticed once again that the fitting by the Gaussian function results in unphysically large values of the spectral temperatures.

The experimental transverse momentum spectra of the negative pions for the analyzed three rapidity ranges in ^{12}C+^{181}Ta collisions at 4.2 GeV/c per nucleon and the corresponding fits in the range p_t = 0.1–1.2 GeV/c by the two-temperature Hagedorn function are shown in Fig. 5. It is important to note that the p_t spectra of the negative pions for different rapidity ranges were normalized per one pion, because pions produced in one collision event may belong to different rapidity regions, i.e., the same collision event may contribute to the p_t spectra of the negative pions from different rapidity intervals. As can be seen from Fig. 5, the p_t spectra of the negative pions in peripheral, semicentral and central ^{12}C+^{181}Ta collisions are fitted very well by the two-temperature Hagedorn function.

To check the influence of the fitting range of p_t on the extracted spectral temperatures T_1 and T_2, the total p_t spectra of the negative pions and the respective spectra of π^- mesons for different ^{12}C+^{181}Ta collision centralities and three rapidity regions considered in this analysis were also fitted in the range p_t = 0.1–0.7 GeV/c. It is necessary to mention that a similar analysis was done in our recent paper,[22] where the centrality and rapidity dependences of transverse momentum spectra of the negative pions produced in ^{12}C+^{12}C collisions at 4.2A GeV/c were investigated. While comparing fit results for p_t = 0.1–0.7 and p_t = 0.1–1.2 GeV/c ranges, it was observed[22] that high p_t ($p_t > 0.7$ GeV/c) and high temperature part of the pion

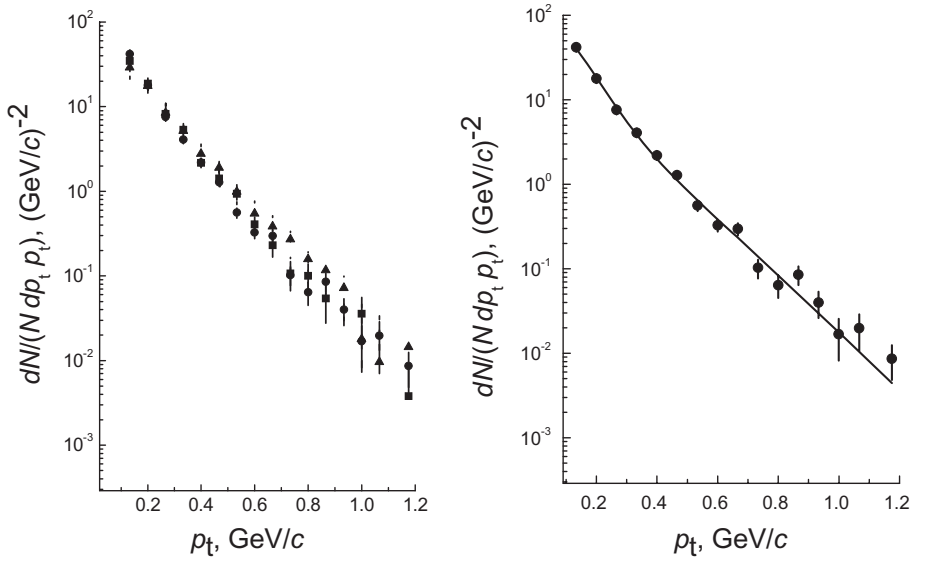

(a) (b)

Fig. 5. The experimental transverse momentum spectra of the negative pions for rapidity range $y_{\rm cm} \leq -0.3$ (•) ((a) and (b)), for rapidity range $|y_{\rm cm.}| \leq 0.3$ (▲) ((a) and (c)), and for rapidity range $y_{\rm cm.} \geq 0.3$ (■) ((a) and (d)) in ^{12}C+^{181}Ta collisions at 4.2 GeV/c per nucleon and the corresponding fits in the range p_t = 0.1–1.2 GeV/c by the two-temperature Hagedorn function (solid lines). All the spectra are normalized per one negative pion.

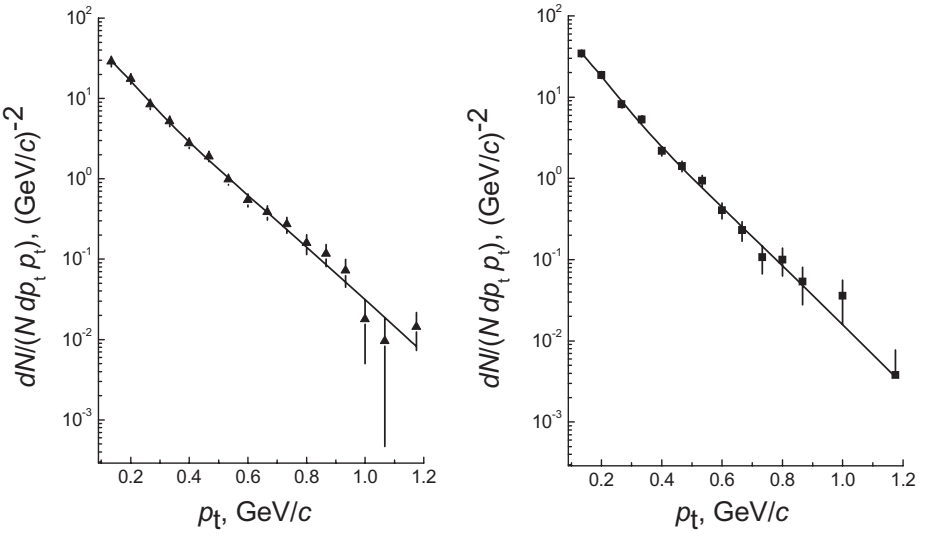

Fig. 5. (*Continued*)

Table 8. Parameters extracted from fitting the total transverse momentum spectra of the negative pions in the range $p_t = 0.1$–$0.7\,\mathrm{GeV}/c$ in $^{12}\mathrm{C}+^{181}\mathrm{Ta}$ collisions at $4.2A\,\mathrm{GeV}/c$ by various two-temperature functions.

Fitting function	A_1	T_1 (MeV)	A_2	T_2 (MeV)	$\chi 2$/n.d.f.	R^2 factor
Hagedorn	$60{,}366 \pm 48{,}300$	44 ± 8	1401 ± 667	108 ± 9	1.01	0.99
Boltzmann	$42{,}464 \pm 26{,}279$	41 ± 6	1038 ± 436	98 ± 7	1.04	0.99
Simple exponential	438 ± 126	67 ± 23	111 ± 112	131 ± 26	0.99	0.99
Gaussian	22 ± 3	353 ± 12	154 ± 18	161 ± 8	1.83	0.99

spectra with quite large statistical errors influences significantly the extracted values of T_1 and T_2, masking and suppressing the centrality dependence of the spectral temperatures. The parameters extracted from fitting the total transverse momentum spectra of the negative pions in the range $p_t = 0.1$–$0.7\,\mathrm{GeV}/c$ in $^{12}\mathrm{C}+^{181}\mathrm{Ta}$ collisions at $4.2A\,\mathrm{GeV}/c$ by the considered two-temperature functions are given in Table 8. From comparison of Tables 4 and 8, one can deduce that the values of the spectral temperatures T_1 and T_2 are consistently lower for the fitting range $p_t = 0.1$–$0.7\,\mathrm{GeV}/c$ compared to the fitting interval $p_t = 0.1$–$1.2\,\mathrm{GeV}/c$. A similar trend was also observed in our recent work.[22] This could be likely due to the reason that the p_t spectra in the former transverse momentum fitting range are lesser affected by the high temperature tail of the pion spectra as compared to the latter fitting range. As expected, Table 8 shows that the values of T_1 and T_2 extracted from fitting with the two-temperature Hagedorn and the two-temperature Boltzmann functions are compatible with each other within the uncertainties.

Table 9. The parameters extracted from fitting the transverse momentum spectra of negative pions in the range $p_t = 0.1$–$0.7\,\mathrm{GeV}/c$ in peripheral, semicentral and central $^{12}\mathrm{C}+^{181}\mathrm{Ta}$ collisions at $4.2A\,\mathrm{GeV}/c$ by various two-temperature functions.

Fitting function	Collision centrality	A_1	T_1 (MeV)	A_2	T_2 (MeV)	$\chi 2$/ n.d.f.	R^2 factor
Hagedorn	Peripheral	$38{,}798 \pm 71{,}350$	38 ± 14	982 ± 506	100 ± 9	0.85	0.99
	Semicentral	$79{,}014 \pm 65{,}917$	45 ± 8	1899 ± 915	111 ± 9	0.54	0.99
	Central	$262{,}592 \pm 329{,}768$	39 ± 9	4224 ± 2391	101 ± 10	1.45	0.99
Boltzmann	Peripheral	$24{,}118 \pm 31{,}482$	36 ± 10	717 ± 348	91 ± 8	0.84	0.99
	Semicentral	$54{,}634 \pm 34{,}661$	43 ± 6	1341 ± 585	102 ± 7	0.51	0.99
	Central	$169{,}975 \pm 165{,}624$	37 ± 7	3094 ± 1590	92 ± 8	1.46	0.99
Simple exponential	Peripheral	156 ± 288	49 ± 51	93 ± 51	116 ± 14	0.91	0.99
	Semicentral	702 ± 361	61 ± 23	215 ± 136	126 ± 15	0.61	0.99
	Central	1352 ± 931	55 ± 27	362 ± 303	119 ± 20	1.49	0.99
Gaussian	Peripheral	13 ± 3	335 ± 15	62 ± 11	153 ± 13	1.01	0.99
	Semicentral	25 ± 5	382 ± 15	222 ± 28	173 ± 9	0.58	0.99
	Central	57 ± 11	333 ± 14	415 ± 69	150 ± 11	1.77	0.98

The parameters extracted from fitting the transverse momentum spectra of the negative pions in the range $p_t = 0.1$–$0.7\,\mathrm{GeV}/c$ in peripheral, semicentral and central $^{12}\mathrm{C}+^{181}\mathrm{Ta}$ collisions at $4.2A\,\mathrm{GeV}/c$ by the above considered two-temperature functions are shown in Table 9. As can be seen from Table 9, the extracted values of the spectral temperatures T_1 and T_2 coincided within the errors for peripheral, semicentral and central $^{12}\mathrm{C}+^{181}\mathrm{Ta}$ collisions when fitted by the two-temperature Hagedorn, Boltzmann and Simple Exponential functions. It is observed from comparison of Tables 6 and 9, that in general the absolute values of T_1 and T_2 are noticeably lower in case of fitting in the range $p_t = 0.1$–$0.7\,\mathrm{GeV}/c$ as compared to the fitting interval $p_t = 0.1$–$1.2\,\mathrm{GeV}/c$. The largest reduction in the extracted spectral temperatures T_1 and T_2 is observed for the p_t spectra of π^- in peripheral collisions when going from fitting in the range $p_t = 0.1$–$1.2\,\mathrm{GeV}/c$ to $p_t = 0.1$–$0.7\,\mathrm{GeV}/c$. This is likely due to the influence of the high temperature p_t part of π^- spectra to the extracted values of T_1 and T_2 in case of the fitting range $p_t = 0.1$–$1.2\,\mathrm{GeV}/c$ compared to the fitting interval $p_t = 0.1$–$0.7\,\mathrm{GeV}/c$.

Table 10 displays the parameters extracted from fitting the transverse momentum spectra of the negative pions in the range $p_t = 0.1$–$0.7\,\mathrm{GeV}/c$ in $^{12}\mathrm{C}+^{181}\mathrm{Ta}$ collisions at $4.2A\,\mathrm{GeV}/c$ by the same two-temperature functions for different pion rapidity intervals. As can be seen from Table 10, the extracted values of the spectral temperatures T_1 and T_2 are consistently larger for the p_t spectra of π^- mesons coming from midrapidity range ($|y_{\mathrm{cm.}}| \leq 0.3$) as compared to the transverse momentum spectra of the negative pions generated in the target ($y_{\mathrm{cm.}} \leq -0.3$) and projectile ($y_{cm.} \geq 0.3$) fragmentation regions. As observed from Table 10, the absolute values of the spectral temperatures T_1 of the negative pions coming from projectile fragmentation region ($y_{\mathrm{cm.}} \geq 0.3$) proved to be consistently larger than the

Table 10. The parameters extracted from fitting the transverse momentum spectra of the negative pions in the range $p_t = 0.1$–$0.7\,\mathrm{GeV}/c$ in $^{12}\mathrm{C}+^{181}\mathrm{Ta}$ collisions at $4.2A\,\mathrm{GeV}/c$ by various two-temperature functions for different pion rapidity intervals.

Fitting function	Rapidity range	A_1	T_1 (MeV)	A_2	T_2 (MeV)	$\chi 2$/n.d.f.	R^2 factor
Hagedorn	$y_{\mathrm{cm.}} \leq -0.3$	$50{,}595 \pm 44{,}736$	39 ± 7	627 ± 303	102 ± 8	1.44	0.99
	$\lvert y_{\mathrm{cm.}} \rvert \leq 0.3$	6199 ± 7228	54 ± 21	445 ± 496	117 ± 22	0.51	0.99
	$y_{\mathrm{cm.}} \geq 0.3$	$12{,}410 \pm 14{,}196$	48 ± 15	593 ± 599	105 ± 17	1.06	0.99
Boltzmann	$y_{cm.} \leq -0.3$	$32{,}851 \pm 23{,}205$	36 ± 5	465 ± 202	93 ± 7	1.49	0.99
	$\lvert y_{\mathrm{cm.}} \rvert \leq 0.3$	5395 ± 4574	49 ± 13	341 ± 302	106 ± 16	0.50	0.99
	$y_{\mathrm{cm.}} \geq 0.3$	9756 ± 8301	44 ± 10	429 ± 364	96 ± 13	1.05	0.99
Simple exponential	$y_{\mathrm{cm.}} \leq -0.3$	266 ± 101	59 ± 17	45 ± 38	126 ± 22	1.37	0.99
	$\lvert y_{\mathrm{cm.}} \rvert \leq 0.3$	91 ± 128	102 ± 82	14 ± 158	166 ± 334	0.57	0.99
	$y_{\mathrm{cm.}} \geq 0.3$	111 ± 105	76 ± 68	48 ± 166	125 ± 69	1.13	0.99
Gaussian	$y_{\mathrm{cm.}} \leq -0.3$	9 ± 2	334 ± 12	77 ± 10	148 ± 8	2.41	0.98
	$\lvert y_{\mathrm{cm.}} \rvert \leq 0.3$	9 ± 2	368 ± 22	40 ± 6	176 ± 16	0.54	0.99
	$y_{\mathrm{cm.}} \geq 0.3$	9 ± 2	350 ± 21	52 ± 7	169 ± 13	1.04	0.99

respective temperatures of the negative pions coming from target fragmentation region ($y_{\mathrm{cm.}} \leq -0.3$). This is, as was already mentioned above, due to the high asymmetry of collision system ($A_{\mathrm{proj}} \ll A_{\mathrm{target}}$) and that pions coming from projectile fragmentation region are produced in first single collisions (interactions) of projectile nucleons with target nucleons, whereas pions coming from target fragmentation are produced mostly at lesser energy transfers in secondary nucleon–nucleon collisions in heavy tantalum nuclei. As seen from comparison of Tables 7 and 10, the extracted absolute values of T_1 and T_2 are generally lower in case of fitting in the range $p_t = 0.1$–$0.7\,\mathrm{GeV}/c$ as compared to the fitting interval $p_t = 0.1$–$1.2\,\mathrm{GeV}/c$. The differences in the spectral temperatures extracted in these two fitting ranges are quite small in case of fitting by the two-temperature Hagedorn and the two-temperature Boltzmann functions, as observed from Tables 7 and 10. As was noticed earlier, the fitting of the p_t spectra of the negative pions with the Gaussian function gives unphysically large values of T_1 and T_2.

3. Summary and Conclusions

The transverse momentum spectra of the negative pions produced in minimum bias $^{12}\mathrm{C}+^{181}\mathrm{Ta}$ collisions at $4.2A\,\mathrm{GeV}/c$ were analyzed by fitting with the four different commonly used functions: Hagedorn, Boltzmann, Simple Exponential and Gaussian functions. It was observed that the p_t spectra of π^- mesons are fitted much better using the two-temperature Hagedorn and Boltzmann functions as compared to the fitting done by the one-temperature functions, which is in agreement with the earlier works.[12–14,16,17,20] Out of the above four fitting functions, Hagedorn and Boltzmann functions provide better fits of the experimental p_t spectra giving the physically acceptable values of the spectral temperatures, compared to the other

two functions. The fitting of the p_t spectra of pions with Boltzmann function gives noticeably lower values of the spectral temperatures compared to that by Hagedorn function. It was observed that the fitting of the pion spectra by Gaussian function is not appropriate, since it gives unphysically large values of T_1 and T_2. The above conclusions confirm the similar findings of our recent paper.[22] The spectral temperatures (T_1, T_2) of π^- mesons in ^{12}C+^{181}Ta collisions at $4.2A\,\mathrm{GeV}/c$ and their relative contributions (R_1, R_2) were extracted from fitting the total p_t spectra in the whole p_t range of π^- by the two-temperature Hagedorn and the two-temperature Boltzmann functions. The dominant contribution ($R_1 \sim 80$–83%) to the total π^- multiplicity in ^{12}C+^{181}Ta collisions at $4.2A\,\mathrm{GeV}/c$ is given by the spectral temperature $T_1 \sim (50\text{–}57) \pm 3\,\mathrm{MeV}$, which is compatible within the uncertainties with the results of Ref. 12. The values of the spectral temperatures (T_1, T_2) extracted in the present work from fitting the p_t spectra by the two-temperature Hagedorn and the two-temperature Boltzmann functions proved to be noticeably lower compared to the corresponding values obtained in Ref. 12 from fitting the noninvariant cm energy spectra of the negative pions by Maxwell–Boltzmann distribution function in ^{12}C+^{181}Ta collisions at $4.2A\,\mathrm{GeV}/c$.

We extracted and fitted the p_t spectra of the negative pions for peripheral, semicentral and central ^{12}C+^{181}Ta collisions as well as for three rapidity regions of π^- in the fitting ranges $p_t = 0.1\text{–}1.2\,\mathrm{GeV}/c$ and $p_t = 0.1\text{–}0.7\,\mathrm{GeV}/c$. In general, the absolute values of T_1 and T_2 were lower in case of fitting in the range $p_t = 0.1\text{–}0.7\,\mathrm{GeV}/c$ as compared to the fitting interval $p_t = 0.1\text{–}1.2\,\mathrm{GeV}/c$. The extracted values of the spectral temperatures T_1 and T_2 were consistently larger for the p_t spectra of π^- mesons coming from midrapidity range ($|y_{\mathrm{cm.}}| \leq 0.3$) as compared to those of transverse momentum spectra of the negative pions generated in the target ($y_{\mathrm{cm.}} \leq -0.3$) and projectile ($y_{\mathrm{cm.}} \geq 0.3$) fragmentation regions. The spectral temperatures of the negative pions coming from projectile fragmentation region ($y_{\mathrm{cm.}} \geq 0.3$) proved to be consistently larger compared to the respective temperatures of the negative pions coming from target fragmentation region ($y_{\mathrm{cm.}} \leq -0.3$). The extracted spectral temperatures T_1 and T_2 of the p_t spectra of π^- mesons were compatible within the uncertainties for the group of peripheral, semicentral and central ^{12}C+^{181}Ta collision events, selected using the number of participant protons in collision events.

Acknowledgments

We express our gratitude to the staff of the Laboratory of High Energies of JINR (Dubna, Russia) and of the Laboratory of Multiple Processes of Physical-Technical Institute of Uzbek Academy of Sciences (Tashkent, Uzbekistan), who took part in the processing of stereophotographs from 2 m propane bubble chamber of JINR. Imran Khan is grateful to the Higher Education Commission (HEC) of Pakistan for financial support under IPFP project. This paper was partially supported by HEC (Higher Education Commission of Pakistan) Research Project N 1925.

References

1. D. Krpic, G. Skoro, I. Picuric, S. Backovic and S. Drndarevic, *Phys. Rev. C* **65** (2002) 034909.
2. Kh. K. Olimov, *Phys. Rev. C* **76** (2007) 055202.
3. Kh. K. Olimov, S. L. Lutpullaev, B. S. Yuldashev, Y. H. Huseynaliyev and A. K. Olimov, *Eur. Phys. J. A* **44** (2010) 43.
4. Kh. K. Olimov, *Phys. At. Nucl.* **73** (2010) 433.
5. Kh. K. Olimov *et al.*, *Phys. Rev. C* **75** (2007) 067901.
6. Kh. K. Olimov and M. Q. Haseeb, *Eur. Phys. J. A* **47** (2011) 79.
7. K. K. Olimov, M. Q. Haseeb, A. K. Olimov and I. Khan, *Centr. Eur. J. Phys.* **9** (2011) 1393.
8. Kh. K. Olimov, M. Q. Haseeb, I. Khan, A. K. Olimov and V. V. Glagolev, *Phys. Rev. C* **85** (2012) 014907.
9. Kh. K. Olimov, M. Q. Haseeb and I. Khan, *Phys. At. Nucl.* **75** (2012) 479.
10. E814 Collab. (J. Barette *et al.*), *Phys. Lett. B* **351** (1995) 93.
11. G. E. Brown, J. Stachel and G. M. Welke, *Phys. Lett. B* **253** (1991) 19.
12. S. Backovic *et al.*, *Phys. Rev. C* **46** (1992) 1501.
13. Kh. K. Olimov, M. Q. Haseeb and S. A. Hadi, *Int. J. Mod. Phys. E* **22** (2013) 1350020.
14. R. Brockmann *et al.*, *Phys. Rev. Lett.* **53** (1984) 2012.
15. L. Chkhaidze *et al.*, *Z. Phys. C* **54** (1992) 179.
16. B. Li and W. Bauer, *Phys. Rev. C* **44** (1991) 450.
17. L. Chkhaidze, T. Djobava and L. Kharkhelauri, *Bull. Georg. Natl. Acad. Sci.* **4** (2010) 41.
18. L. Chkhaidze *et al.*, *Nucl. Phys. A* **831** (2009) 22.
19. R. Hagedorn and J. Rafelski, *Phys. Lett. B* **97** (1980) 136.
20. Kh. K. Olimov and M. Q. Haseeb, *Phys. At. Nucl.* **76** (2013) 595.
21. Kh. K. Olimov, A. Iqbal, V. V. Glagolev and M. Q. Haseeb, *Phys. Rev. C* **88** (2013) 064903.
22. A. Iqbal *et al.*, *Int. J. Mod. Phys. E* **23** (2014) 1450047.
23. Lj. Simic *et al.*, *Phys. Rev. C* **52** (1995) 356.
24. A. I. Bondarenko *et al.*, *Phys. At. Nucl.* **65** (2002) 90.
25. L. Chkhaidze, T. Djobava and L. Kharkhelauri, *Bull. Georg. Natl. Acad. Sci.* **6** (2012) 44.
26. K. Olimov, S. L. Lutpullaev, A. K. Olimov, V. I. Petrov and S. A. Sharipova, *Phys. At. Nucl.* **73** (2010) 1847.
27. L. Chkhaidze, P. Danielewicz, T. Djobava, L. Kharkhelauri and E. Kladnitskaya, *Nucl. Phys. A* **794** (2007) 115.
28. G. N. Agakishiyev *et al.*, *Z. Phys. C* **27** (1985) 177.
29. D. Armutlisky *et al.*, *Z. Phys. A* **328** (1987) 455.
30. A. I. Bondarenko *et al.*, JINR Preprint No. P1-98-292 (JINR, Dubna, 1998).
31. V. D. Toneev, N. S. Amelin, K. K. Gudima and S. Yu. Sivoklokov, *Nucl. Phys. A* **519** (1990) 463c.
32. N. S. Amelin, K. K. Gudima, S. Yu. Sivoklokov and V. D. Toneev, *Sov. J. Nucl. Phys.* **52** (1990) 172.
33. N. S. Amelin, K. K. Gudima and V. D. Toneev, *Sov. J. Nucl. Phys.* **51** (1990) 1093.
34. N. S. Amelin, E. F. Staubo, L. P. Csernai, V. D. Toneev and K. K. Gudima, *Phys. Rev. C* **44** (1991) 1541.
35. B. Gankhuyag and V. V. Uzhinskii, JINR Preprint No. P2-96-419 (JINR, Dubna, 1996).

36. A. S. Galoyan, G. L. Melkumov and V. V. Uzhinskii, *Phys. Atom. Nucl.* **65** (2002) 1722.
37. A. S. Galoyan *et al.*, *Phys. Atom. Nucl.* **66** (2003) 836.
38. Ts. Baatar *et al.*, *Phys. Atom. Nucl.* **63** (2000) 839.
39. R. Hagedorn and J. Ranft, *Suppl. Nuovo Cimento* **6** (1968) 169.
40. NA44 Collab. (I. Bearden *et al.*), *Phys. Rev. Lett.* **78** (1997) 2080.
41. L. Chkhaidze *et al.*, *Phys. Rev. C* **84** (2011) 064915.
42. L. V. Chkhaidze *et al.*, *Phys. Atom. Nucl.* **67** (2004) 693.
43. S. Backovic *et al.*, *Sov. J. Nucl. Phys.* **50** (1989) 1001.